Water Promoted One Pot Synthesis of Sesamol Derivatives as Potent Antioxidants: DFT, Molecular Docking, SAR and Single Crystal Studies

Jaydeep N. Lalpara, Sanjay D. Hadiyal, B. B. Dhaduk, Maneesh Kumar Gupta, M. B. Solanki, Ashoke Sharon & G. G. Dubal

Published online: 03 Jun 2022.

Submit your article to this journal

View related articles

View Crossmark data

Taylor & Francis
Taylor & Francis Group

Check for updates

Water Promoted One Pot Synthesis of Sesamol Derivatives as Potent Antioxidants: DFT, Molecular Docking, SAR and Single Crystal Studies

Jaydeep N. Lalpara[a] (ID), Sanjay D. Hadiyal[a] (ID), B. B. Dhaduk[b], Maneesh Kumar Gupta[c], M. B. Solanki[d], Ashoke Sharon[e] (ID), and G. G. Dubal[a] (ID)

aDepartment of Chemistry, RK University, Rajkot, Gujarat, India; bDepartment of Chemistry, Atmiya University, Rajkot, Gujarat, India; cDepartment of Chemistry, Hotilal Ramnath College (A Constituent Unit of Jai Prakash University), Amnour, Chapra, Bihar, India; dSchool of Technology, Pandit Deendayal Petroleum University, Gandhinagar, India; eBirla Institute of Technology, Mesra, Ranchi, India

ABSTRACT

A one pot water mediated synthesis of sesamol analogous using Betti Base synthetic approach. The reaction was optimized with various solvents and catalysts, but the product formed with a high yield in aqueous ethanol condition. The examined strategy offers many advantages such as green solvent, purification without column chromatography, and catalyst-free synthesis. The synthesized molecules were investigated for molecular docking and DFT studies. In silico parameter showed that the compound **4h** has the lowest affinity score as well as high charge transformations. From the result of theoretical approaches, we evaluate compounds for *in vitro* antioxidant assay toward the DPPH, H_2O_2 and NO method with $50\,\mu g/mL$ concentration. In vitro bioassay revealed that the compound 4 h had excellent inhibition capacity.
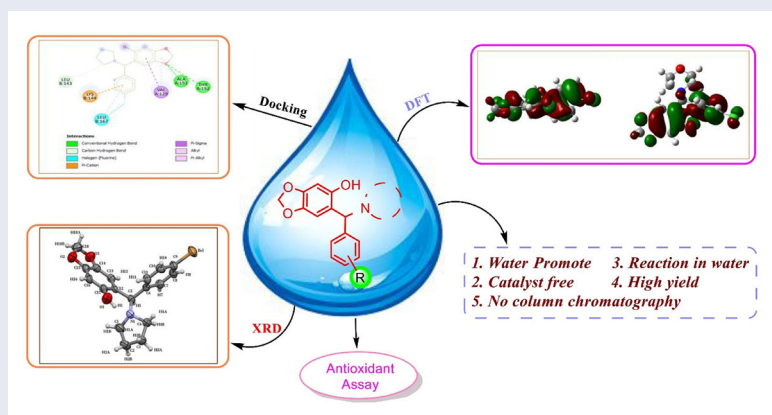
1. Introduction

Due to its biradical nature, molecular oxygen can easily accept electrons, thereby producing a series of partially reduced substances, collectively referred to as reactive oxygen species (ROS). Some of the radicals such as anions of superoxide ($O_2^{\bullet-}$), peroxyl radicals ($ROO^\bullet$), hydrogen peroxide, alkoxyl radicals ($RO^\bullet$), and hydroxyl radicals ($HO^\bullet$). They are often intricate in the beginning

and propagation of chain reactions that are very harmful to cells.[1–3] Oxidative stress (OS) is the result of unfettered ROS production and the imbalance of antioxidant homeostasis leading to the formation of toxic ROS.[4,5] Oxidative stress (OS) performs a significant role in neurodegenerative diseases such as Alzheimer's disease, amyotrophic lateral sclerosis,[6–8] Parkinson's disease, vascular diseases, diabetic disease,[9,10] and rheumatoid arthritis, and cancer.[11] Additionally, they are used as food additives, especially to prevent rancidity, antioxidants can effectively in protecting cells or tissues from oxidative damage as well as protectors against aging, poisoning by toxic agents.[12–14]

Sesame is an important oilseed extracted from *Sesamum indicum*. It is one of the oldest oil seeds known to mankind. It not only has nutritional value but also has medicinal value. Sesame oil contains several trace components including sesamin, sesamolin, and sesamol.[15–17] The antioxidant is one of the most studied properties of sesamol.[18–21] It has been proven to effectively inhibit the degradation of deoxyribose and lipid peroxidation induced by hydroxyl free radicals, which helps protect plasma, low-density lipoproteins, and red blood cell membranes from oxidation.[22–24] Sesamol has been proven to be an anti-aging agent, which can prevent light damage caused by long-term ultraviolet radiation, exhibit anti-mutagenic effects, and is a plasminogen activator that prevents atherosclerosis. It has also been studied for the treatment of various diseases.[25–28]

Many syntheses have been carried out using green chemistry principles.[29–32] Our endless efforts to design biologically active heterocycles toward various biological responses.[33–37] The attractive properties of sesamol have gained our attraction on the possible application of its derivatives for various purposes. We reported some newly designed molecules for various activity purposes but herein we wish to report some sesamol incorporated derivatives with the green chemistry approach.

2. Materials and methods

2.1. General information

All chemicals and solvents were purchased from Sigma Aldrich and SRL. All purchased chemicals were used without further purification, reaction progress was continuously monitored by thin-layer chromatography (TLC) on silica gel-(G60 F254) of 0.5 mm thickness, visualizing with ultraviolet light (254 and 365 nm), or with iodine vapor. Melting points were determined using a Buchi B-540 capillary apparatus. NMR spectra were recorded on a Bruker Advance 400 MHz spectrometer (400 MHz for ^{1}H NMR and 101 MHz for ^{13}C NMR), respectively, in solvents like CDCl$_3$, DMSO-d_6, and chemical shifts are referenced to the solvent residual signals to tetramethylsilane. Standard abbreviations are used to represent signal multiplicities for ^{1}H NMR spectrum singlet (s), doublet (d), triplet (t), quartet (q), and multiplate (m). Mass spectra were recorded on a Shimadzu GC-MSQP-2010 mass spectrometer in EI (70 eV) model using the direct inlet probe technique and m/z is reported in atomic units per elementary charge. X-ray diffraction analysis was performed on a Rigaku SXC mini.

2.2. General procedure for the synthesis of sesamol derivatives (4a–j)

To aqueous ethanol (1:1) (6 mL) containing RBF, pyrrolidine/morpholine/piperidine (1 mmol) (2) and substituted aromatic aldehyde (1.2 mmol) (3a–j) were added and allowed to stir for 10-15 min at room temperature to form imine like intermediate. After that, the addition of sesamol (1 mmol) (1) into RBF allowed reflux for 6–8 h. The reaction progress was continuously monitored by TLC. After completion of the reaction, the reaction mixture was poured into ice crushed water to get a crude product. The crude product was triturated with *n*-hexane and diethyl ether to get pure product and dry it (4a–j). Compounds were recrystallized with ethyl acetate.

2.3. Spectral analysis

6-((4-bromophenyl)(morpholino)methyl)benzo[d][1,3]dioxol-5-ol **(4a)**. ^{1}H-NMR (400 MHz, CDCl$_3$): δ_{ppm} 2.44 (d, $J = 5.2$ Hz, 4 H$_{aliphatic}$, CH$_2$), 3.77 (s, 4 H$_{aliphatic}$, CH$_2$), 4.23 (t, $J = 6.0$ Hz, 1 H$_{chiral}$, CH), 5.81-5.88 (m, 2 H, OCH$_2$), 6.37-6.45 (m, 2 H$_{aromatic}$), 7.28-7.48 (m, 4 H$_{aromatic}$), 11.48 (s, 1 H, -OH); ^{13}C-NMR (101 MHz, CDCl$_3$): δ_{ppm} 31.82, 39.14, 50.29, 51.61, 62.07, 89.49, 104.84, 124.40, 127.99, 129.21, 143.05, 149.70, 163.75, 164.31; MS (EI, 70 eV) m/z: 394.8 (M + 2). Anal. Calcd. for C$_{18}$H$_{18}$BrNO$_4$: C, 55.12%; H, 4.63%; N, 3.57%; Found: C, 52.12%; H, 4.59%; N, 3.58%.

6-((4-chlorophenyl)(morpholino)methyl)benzo[d][1,3]dioxol-5-ol **(4b)**. ^{1}H-NMR (400 MHz, DMSO-d_6): δ_{ppm} 1.73 (s, 4 H$_{aliphatic}$, CH$_2$), 2.34 (d, $J = 0.8$ Hz, 4 H$_{aliphatic}$, CH$_2$), 4.65 (s, 1 H$_{chiral}$, CH), 5.84 (d, $J = 14$ Hz, 2 H, OCH$_2$), 6.35 (s, 1 H$_{aromatic}$), 6.88 (s, 1 H$_{aromatic}$), 7.68 (d, $J = 8.8$ Hz, 2 H$_{aromatic}$), 8.14 (d, $J = 8.8$ Hz, 2 H$_{aromatic}$), 10.02 (s, 1 H, -OH); ^{13}C-NMR (101 MHz, DMSO-d_6): δ_{ppm} 48.38, 65.19, 74.52, 99.85, 100.61, 111.75, 130.42, 132.47, 134.10, 139.83, 142.36, 150.72, 156.52; MS (EI, 70 eV) m/z: 349.62 (M + 2). Anal. Calcd. for C$_{18}$H$_{18}$ClNO$_4$: C, 62.16%; H, 5.22%; N, 4.03%; Found: C, 62.19%; H, 5.19%; N, 4.11%.

6-((4-fluorophenyl)(morpholino)methyl)benzo[d][1,3]dioxol-5-ol **(4c)**. ^{1}H-NMR (400 MHz, DMSO-d_6): δ_{ppm} 1.72 (s, 4 H$_{aliphatic}$, CH$_2$), 2.34 (d, $J = 6$ Hz, 2 H$_{aliphatic}$, CH$_2$), 2.43 (d, $J = 8.8$ Hz, 2 H$_{aliphatic}$, CH$_2$), 4.50 (s, 1 H$_{chiral}$, CH), 5.84 (q, $J = 8.4$ Hz, 2 H, OCH$_2$), 6.15 (s, 1 H$_{aromatic}$), 6.34 (s, 1 H$_{aromatic}$), 6.81 (s, 1 H$_{aromatic}$), 7.28-7.44 (m, 3 H$_{aromatic}$), 10.30 (s, 1 H, OH); ^{13}C-NMR (101 MHz, DMSO-d_6): δ_{ppm} 50.53, 64.71, 73.66, 100.87, 103.72, 109.87, 116.51, 122.74, 130.34, 135.43, 142.25, 148.36, 156.50, 162.39; MS (EI, 70 eV) m/z: 333.54 (M + 2). Anal. Calcd. for C$_{18}$H$_{18}$FNO$_4$: C, 65.25%; H, 5.48%; N, 4.23%; Found: C, 63.04%; H, 5.37%; N, 4.10%.

6-((3,4-dimethoxyphenyl)(morpholino)methyl)benzo[d][1,3]dioxol-5-ol **(4d)**. ^{1}H-NMR (400 MHz, CDCl$_3$): δ_{ppm} 2.38-2.45 (m, 2 H$_{aliphatic}$, CH$_2$), 2.60 (s, 2 H$_{aliphatic}$, CH$_2$), 3.75 (t, $J = 6.4$ Hz, 4 H$_{aliphatic}$, CH$_2$), 3.84 (s, 6 H, CH$_3$), 4.19 (s, 1 H$_{chiral}$, CH), 5.81 (dd, $J = 2$ Hz, 1.6 Hz, 2 H, OCH$_2$), 6.40 (d, $J = 10.8$ Hz, 2 H$_{aromatic}$), 6.78 (d, $J = 10.8$ Hz, 2 H$_{aromatic}$), 6.93 (t, $J = 10.8$ Hz, 2 H$_{aromatic}$), 11.64 (s, 1 H, OH); ^{13}C-NMR (101 MHz, CDCl$_3$): δ_{ppm} 46.58, 57.78, 73. 42, 98.61, 101.13, 110.66, 114.43, 113.86, 121.35, 124.19, 130.57, 142.48, 149.93, 150.58, 156.84; MS (EI, 70 eV) m/z: 374.71 (M + 1). Anal. Calcd. for C$_{20}$H$_{23}$NO$_6$: C, 64.33%; H, 6.21%; N, 3.75%; Found: C, 64.31%; H, 6.13%; N, 3.76%.

6-(morpholino(4-nitrophenyl)methyl)benzo[d][1,3]dioxol-5-ol **(4e)**. ^{1}H-NMR (300 MHz, CDCl$_3$): δ_{ppm} 2.40-2.46 (m, 2 H$_{aliphatic}$, CH$_2$), 2.63 (s, 2 H$_{aliphatic}$, CH$_2$), 3.76 (t, $J = 4.5$ Hz, 4 H$_{aliphatic}$, CH$_2$), 4.34 (s, 1 H$_{chiral}$, CH), 5.83 (dd, $J = 14.4$ Hz, 2 H, OCH$_2$), 6.39 (d, $J = 13.5$ Hz, 2 H$_{aromatic}$), 7.61 (d, $J = 8.7$ Hz, 2 H$_{aromatic}$), 8.17 (d, $J = 9$ Hz, 2 H$_{aromatic}$), 11.18 (s, 1 H, OH); ^{13}C-NMR (75 MHz, CDCl$_3$): δ_{ppm} 53.11, 65.89, 78.24, 98.37, 102.43, 113.04, 115.19, 125.71, 127.45, 142.27, 146.38, 149.56, 155.53; MS (EI, 70 eV) m/z: 359.48 (M + 1). Anal. Calcd. for C$_{18}$H$_{18}$N$_2$O$_6$: C, 60.33%; H, 5.06%; N, 7.82%; Found: C, 60.18%; H, 4.92%; N, 7.87%.

6-((4-bromophenyl)(pyrrolidin-1-yl)methyl)benzo[d][1,3]dioxol-5-ol **(4f)**. ^{1}H-NMR (400 MHz, CDCl$_3$): δ_{ppm} 1.81-1.84 (m, 4 H$_{alipatic}$, CH$_2$), 2.46 (d, $J = 6$ Hz, 2 H$_{alipatic}$, CH$_2$), 2.62 (s, 2 H$_{alipatic}$, CH$_2$), 4.18 (s, 1 H$_{chiral}$, CH), 5.80 (dd, J = 21.6 Hz, 2 H, OCH$_2$), 6.39 (d, $J = 9.6$ Hz, 2 H$_{aromatic}$), 7.25-7.42 (m, 4 H$_{aromatic}$), 12.06 (s, 1 H, OH); ^{13}C-NMR (101 MHz, CDCl$_3$): δ_{ppm} 20.82, 52.21, 71.14, 81.57, 98.28, 100.09, 109.88, 124.39, 127.96, 129.28, 140.53, 142.86, 149.63, 151.09, 163.66, 164.57; MS (EI, 70 eV) m/z: 378.34 (M + 2). Anal. Calcd. for C$_{18}$H$_{18}$BrNO$_3$: C, 57.46%; H, 4.82%; N, 3.72%; Found: C, 57.26%; H, 4.88%; N, 3.81%.

6-((4-chlorophenyl)(pyrrolidin-1-yl)methyl)benzo[d][1,3]dioxol-5-ol **(4g)**. ^{1}H-NMR (400 MHz, DMSO-d_6): δ_{ppm} 1.728 (s, 4 H$_{aliphatic}$, CH$_2$), 2.34-2.49 (m, 4 H$_{aliphatic}$, CH$_2$), 4.52 (s, 1 H$_{chiral}$, CH), 5.84 (d, $J = 4.8$ Hz, 2 H, OCH$_2$), 6.35 (s, 1 H$_{aromatic}$), 6.84 (s, 1 H$_{aromatic}$), 7.02 (q, $J = 8$ Hz, 1 H$_{aromatic}$), 7.20-7.32 (m, 3 H$_{aromatic}$), 10.37 (s, 1 H, OH); ^{13}C-NMR (101 MHz, DMSO-d_6): δ_{ppm} 25.19, 52.94, 77.67, 99.91, 101.28, 111.63, 122.75, 131.56, 132.33, 133.82, 139.26, 143.49, 150.62,

156.30; MS (EI, 70 eV) m/z: 333.4 (M + 2). Anal. Calcd. for $C_{18}H_{18}ClNO_3$: C, 65.16%; H, 5.47%; N, 4.22%; Found: C, 65.32%; H, 5.35%; N, 4.23%.

6-((4-fluorophenyl)(pyrrolidin-1-yl)methyl)benzo[d][1,3]dioxol-5-ol **(4h)**. ^{1}H-NMR (300 MHz, CDCl$_3$): δ_{ppm} 1.89 (t, $J = 6.2$ Hz, 4 H$_{aliphatic}$, CH$_2$), 2.43 (t, $J = 6$ Hz, 2 H$_{aliphatic}$, CH$_2$), 2.64 (s, 2 H$_{aliphatic}$, CH$_2$), 4.22 (s, 1 H$_{chiral}$, CH), 5.81 (q, $J = 12.4$ Hz, 2 H, OCH$_2$), 6.39 (m, 2 H$_{aromatic}$), 6.95 (m, 2 H$_{aromatic}$), 7.44 (m, 2 H$_{aromatic}$), 9.67 (s, 1 H, OH); ^{13}C-NMR (75 MHz, CDCl$_3$): δ_{ppm} 23.29, 52.17, 72.53, 99.82, 101.75, 108.68, 117.56, 118.84, 129.91, 138.16, 141.08, 148.19, 151.25, 161.46, 163.88; MS (EI, 70 eV) m/z: 317.39 (M + 2). Anal. Calcd. for $C_{18}H_{18}FNO_3$; C, 68.56%; H, 5.75%; N, 4.44%; Found; C, 68.74%; H, 5.53%; N, 4.41%.

6-((4-nitrophenyl)(pyrrolidin-1-yl)methyl)benzo[d][1,3]dioxol-5-ol **(4i)**. ^{1}H-NMR (300 MHz, CDCl$_3$): δ_{ppm} 2.39-2.44 (m, 4 H$_{aliphatic}$, CH$_2$), 2.65 (s, 2 H$_{aliphatic}$, CH$_2$), 3.72 (t, $J = 6.2$ Hz, 2 H$_{aliphatic}$, CH$_2$), 4.29 (s, 1 H$_{chiral}$, CH), 5.75 (dd, $J = 12$ Hz, 2 H, OCH$_2$), 6.39 (m, 2 H$_{aromatic}$), 7.53 (d, $J = 8$ Hz, 2 H$_{aromatic}$), 8.22 (d, $J = 9.4$ Hz, 2 H$_{aromatic}$), 10.86 (s, 1 H, OH); ^{13}C-NMR (75 MHz, CDCl$_3$): δ_{ppm} 22.52, 56.71, 77.43, 99.36, 101.28, 112.55, 114.39, 126.04, 130.56, 140.92, 147.18, 148.83, 151.31; MS (EI, 70 eV) m/z: 343.29 (M + 1). Anal. Calcd. for $C_{18}H_{18}N_2O_5$; C, 63.15%; H, 5.30%; N, 8.18%; Found: C, 63.21%; H, 5.27%; N, 8.24%.

6-((4-chlorophenyl)(piperidin-1-yl)methyl)benzo[d][1,3]dioxol-5-ol **(4j)**. ^{1}H-NMR (400 MHz, CDCl$_3$): δ_{ppm} 1.48 (s, 2 H$_{aliphatic}$, CH$_2$), 1.64 (t, $J = 4.8$ Hz, 6 H$_{aliphatic}$, CH$_2$), 2.38 (s, 2 H$_{aliphatic}$, CH$_2$), 4.31 (s, 1 H$_{chiral}$, CH), 5.82 (q, $J = 14.4$ Hz, 2 H, OCH$_2$), 6.32 (s, 1 H$_{aromatic}$), 6.43 (s, 1 H$_{aromatic}$), 7.30 (t, $J = 10$ Hz, 3 H$_{aromatic}$), 12.30 (s, 1 H, OH); ^{13}C-NMR (101 MHz, DMSO-d_6): δ_{ppm} 13.99, 66.05, 112.33, 115.19, 123.59, 123.72, 128.80, 129.00, 129.12, 137.88, 139.13, 148.62, 149.15; MS (EI, 70 eV) m/z: 347.25 (M + 2). Anal. Calcd. for $C_{19}H_{20}ClNO_3$: C, 65.99%; H, 5.83%; N, 4.05%; Found: C, 65.82%; H, 5.87%; N, 4.11%.

2.4. Antioxidant assay

The synthesized compounds **4a–j** were evaluated for their free radical scavenging capacity. The antioxidant activity was carried out toward 2,2-diphenyl-1-picrylhydrazyl (DPPH), hydrogen peroxide (H$_2$O$_2$), and nitric oxide (NO) method.[38–42] All obtained results were compared with the reference drug ascorbic acid.

2.5. Molecular docking

Molecular docking was utilized to explain the binding mode of the ligand to deliver easy information for optimization in structure. Molecular docking is a valuable tool to establish the possible drug-receptor interaction which might be responsible for the biological response. Ascorbic acid is known to bind with the active sites of DPPH. The crystal structure of HORF6 (PDB ID: 1PRX) was selected for the docking study. The 3-D structure of targeted molecules was drawn using ChemDraw and the structures of the drugs were downloaded from the Protein Data Bank (http://www.rcsb.org). The synthesized molecules were then subjected to interact with the receptor through molecular docking using AutoDock Vina.[43] The protocol simplifies flexible compound docking for different compound conformers within the rigid receptor. The best conformation for each compound was chosen and the interaction was visualized in Discovery studio.

2.6. Density functional theory (DFT)

The HOMO and LUMO energy calculated by B3LYP and HF using 6-311++G(d,p) methods are shown. This electronic transition absorption corresponds to the transition from the ground to the first excited state and is mainly described by an electron excitation from the HOMO to the LUMO. The calculation of atomic charges plays an important role in the application of quantum

mechanical calculations to molecular systems.[44] Our interest here is in the comparison of different methods to describe the electron distribution in 2EIDZ as broadly as possible and assess the sensitivity of the calculated charges to changes in (i) the choice of the basis set; (ii) the choice of the quantum mechanical method. Mulliken charges are calculated by determining the electron population of each atom as defined in the basic functions. The Mulliken charges are calculated at different levels and the same basis set is listed. The corresponding Mulliken's plot with different HF and B3LYP with 6-311++G(d,p) methods. The obtained results are mentioned in Table 4. Apart from that electrostatic potential energy, bond length, and Mulliken charges are projected in supporting data.

2.7. Single crystal study

A colorless crystal of $C_{18}H_{18}BrNO_3$ having approximate dimensions of $0.390 \times 0.370 \times 0.160$ mm was mounted on a glass fiber. All measurements were made on a Rigaku SCX mini diffractometer using graphite monochromate Mo-Kα radiation. The crystal-to-detector distance was 52.00 mm. The data were collected at a temperature of $20 \pm 1\,°C$ to a maximum 2θ value of $55.0°$. A total of 540 oscillation images were collected. A sweep of data was done using ω oscillations from -120.0 to $60.0°$ in $1.0°$ steps. The exposure rate was 10.0 [sec./°]. The detector swing angle was $-30.80°$. A second sweep was performed using ω oscillations from -120.0 to $60.0°$ in $1.0°$ steps. The exposure rate was 10.0 [sec./°]. The detector swing angle was $-30.80°$. Another sweep was performed using ω oscillations from -120.0 to $60.0°$ in $1.0°$ steps. The exposure rate was 10.0 [sec./°]. The detector swing angle was $-30.80°$. The crystal-to-detector distance was 52.00 mm. The readout was performed in the 0.146 mm pixel mode.

Data reduction of the 23187 reflections that were collected, 10492 were unique (Rint = 0.0640); equivalent reflections were merged. Data were collected and processed using Crystal Clear (Rigaku). The linear absorption coefficient, μ, for Mo–Kα radiation is $0.871\,cm^{-1}$. An empirical absorption correction was applied which resulted in transmission factors ranging from 0.516 to 0.986. The data were corrected for Lorentz and polarization effects. The structure was solved by direct methods and expanded using Fourier techniques. The non-hydrogen atoms were refined anisotropically. Some hydrogen atoms were refined isotropically and the rest were refined using the riding model. The final cycle of full-matrix least-squares refinement on F^2 was based on 10492 observed reflections and 1026 variable parameters and converged.

The standard deviation of observation of unit weight was 12.24. Unit weights were used. The maximum and minimum peaks on the final difference Fourier map corresponded to 1476.84 and $0.00\ e^-/Å^3$, respectively. The absolute structure was deduced based on the Flack parameter, 0.000, using 4887 Friedel pairs. Neutral atom scattering factors were taken from Cromer and Waber. Anomalous dispersion effects were included in Fcalc; the values for $\Delta f'$ and f'' were those of Creagh and McAuley. The values for the mass attenuation coefficients are those of Creagh and Hubbell. All calculations were performed using the Crystal Structure crystallographic software package except for refinement, which was performed using SHELXL-97.[45]

3. Results and discussion

3.1. Chemistry

The preparation of sesamol derivatives was achieved by the Betti base reaction between secondary amines, aromatic substituted aldehyde and sesamol as a phenolic compound. First, the imine formation by the reaction between secondary amines and aromatic aldehydes. Further, it reacts with a phenolic compound as sesamol and gets the final chiral adducts (Scheme 1). The reaction condition was optimized under various solvent and catalytic conditions (Table 1).

Table 1. Reaction optimization toward compound **4i**.
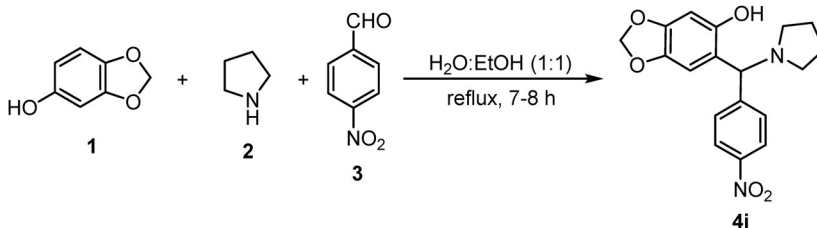
Entry	Catalyst	Solvent	Temp. oC	Time (hr)	% Yield
1	–	MeOH	Reflux	8.0	52
2	–	EtOH	Reflux	8.0	79
3	TBAB (0.5 eq)	THF	Reflux	6.0	35
4	–	H_2O	80	8.0	67
5	–	EtOH: H_2O	Reflux	7.5	76
6	TBAB (0.5 eq)	H_2O	80	9.0	64

Synthesized adducts
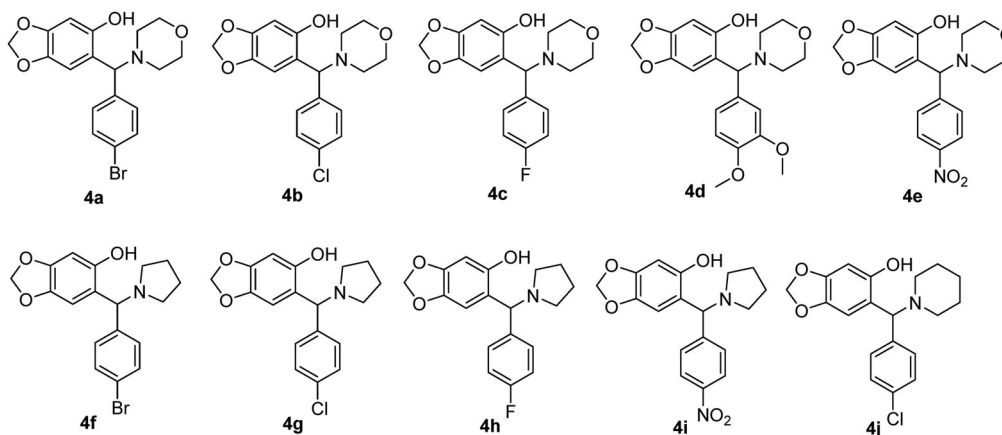
The reaction proceeds with a high yield in polar protic solvent conditions. We did get satisfactory yield in ethanolic conditions whereas the least yield was observed in a polar aprotic solvent such as THF. In efforts toward the green synthesis, we performed the reaction in neat water solvent unfortunately, we found a promising yield. Further, for yield increment, we used phase transfer catalyst (PTC) as TBAB, but we did not find a good yield. Finally, an equivalent mixture of ethanol and water was employed in reaction to achieve final adducts. No column chromatography was used for the purification of final products. All synthesized molecules were purified by a simple trituration method. The crude products were continuously washed with *n*-hexane and diethyl ether. The plausible reaction mechanism is illustrated in Figure 1.

3.2. Biology

The prime attention of an antioxidant is its ability to trap free radicals. The objective of our research is to discover the antioxidant efficacy of compounds **4a-j**, to evolve conspicuous inhibitors. Synthesized compounds were evaluated for their free radical scavenging activities along with ascorbic acid as a standard toward 2,2-diphenyl-1-picrylhydrazyl (DPPH), hydrogen peroxide
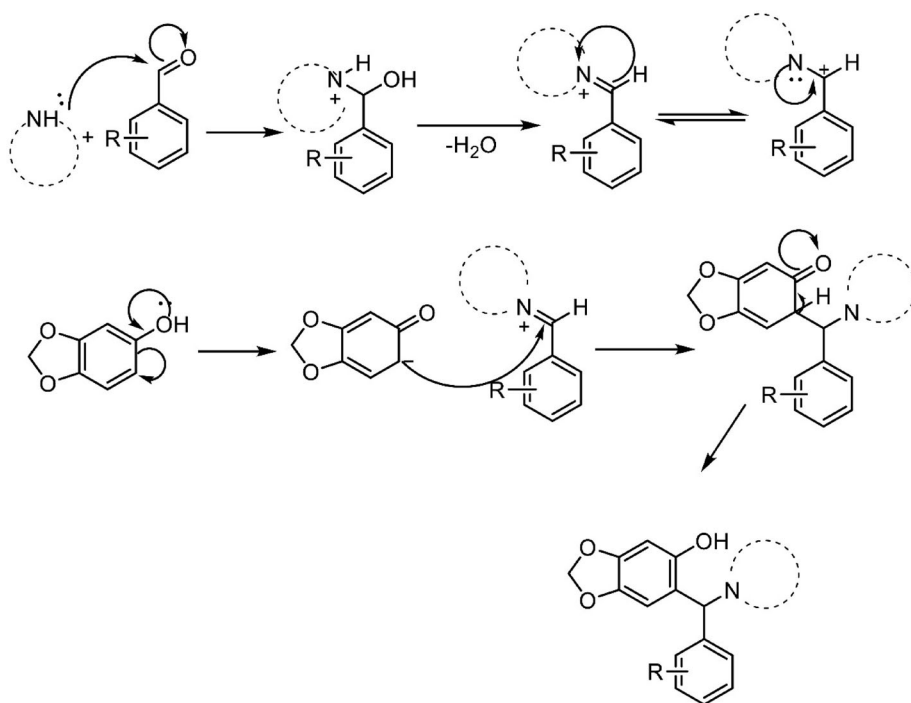
Figure 1. Plausible reaction mechanism for synthesized molecules.

Table 2. Free radical scavenging capacity of compounds **4a–j**.

| | | | 50 μg/mL | |
Entry	Compounds	DPPH	H_2O_2	NO
1	**4a**	**75.48 ± 0.82**	**69.23 ± 0.74**	**76.76 ± 0.15**
2	**4b**	63.69 ± 0.34	62.39 ± 0.60	67.65 ± 0.41
3	**4c**	50.38 ± 0.29	39.10 ± 0.81	51.92 ± 0.93
4	**4d**	49.46 ± 0.33	39.43 ± 1.06	49.36 ± 0.69
5	**4e**	51.74 ± 0.26	41.67 ± 0.38	53.60 ± 0.47
6	**4f**	**75.09 ± 0.65**	**68.91 ± 1.02**	**75.84 ± 0.31**
7	**4g**	67.82 ± 0.54	64.29 ± 0.85	70.25 ± 0.06
8	**4h**	**76.62 ± 0.51**	**70.58 ± 0.11**	**76.33 ± 0.19**
9	**4i**	53.87 ± 0.72	45.39 ± 0.78	52.31 ± 0.10
10	**4j**	54.73 ± 0.37	47.76 ± 1.24	55.88 ± 0.27
11	Ascorbic acid	75.21 ± 0.17	70.62 ± 0.43	77.27 ± 0.08

Bold value signifies highest inhibition.

(H_2O_2) and nitric oxide (NO) method [43-44]. The antioxidant evaluation was performed with fix concentration of 50 μg/mL. Results of free radical scavenging were tabulated in Table 2. From the compounds, Moieties **4a**, **4f**, and **4h** exhibited the greatest antioxidant activity toward the employed methods. The consequences of **4b** and **4g** suggested good activity, while **4d**, **4c**, **4e**, **4i**, and **4j** showed the least activity.

Specifically, motif **4h** was the most inclined compound to control the oxidation with a value of 76.62 ± 0.51 (DPPH), 70.58 ± 0.11 (H_2O_2), and 76.33 ± 0.19 (NO) compared to the standard radical scavenger ascorbic acid. Compare the obtained results with ascorbic acid illustrated in Figure 2.

3.3. SAR between molecular docking, DFT and biological activity results

To examine the mechanism of antioxidant activity and identified the intermolecular interaction between the molecules, docking was performed on the crystal structure of human peroxidase
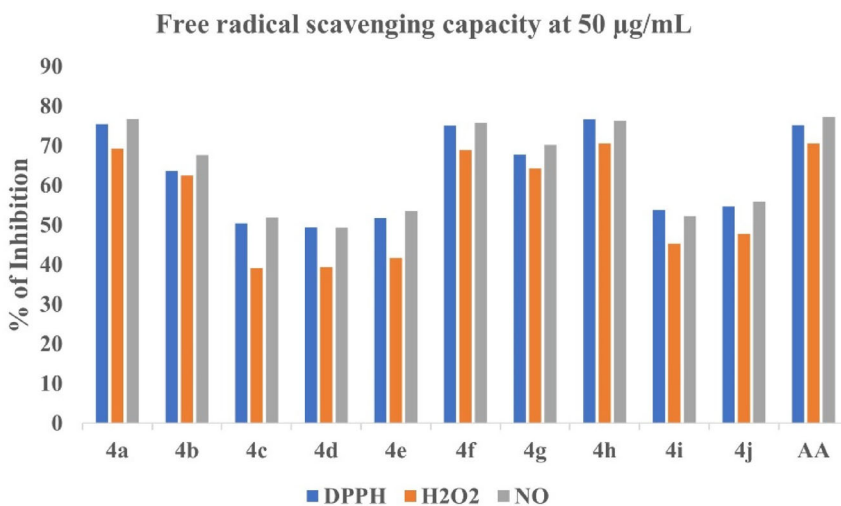
Figure 2. Comparison of % of inhibition toward with applied methods.

Table 3. Dockingscore for compound **4a–j**.

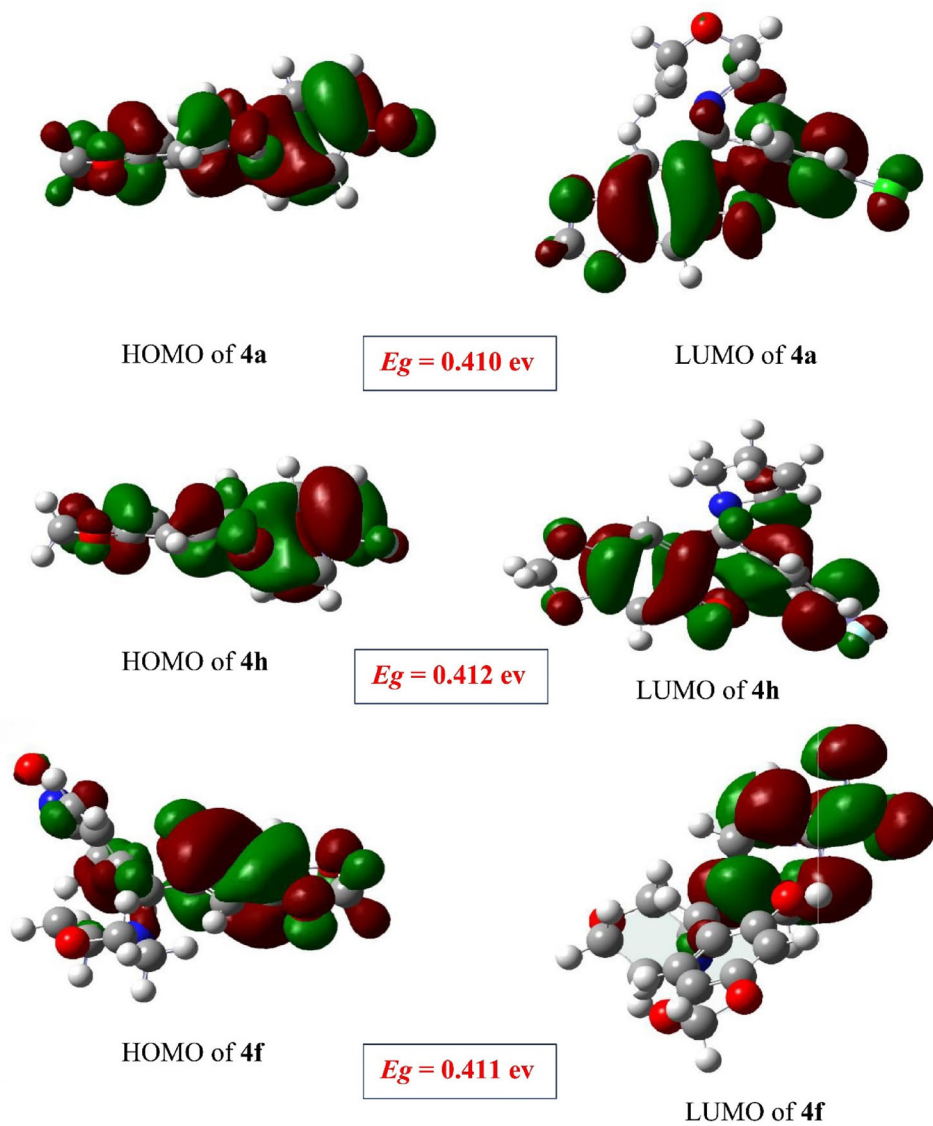| Entry	Ligands	Affinity (kcal/mol)
1	**4a**	−6.7
2	**4b**	−6.4
3	**4c**	−6.7
4	**4d**	−6.3
5	**4e**	−6.3
6	**4f**	−6.7
7	**4g**	−6.5
8	**4h**	−6.8
9	**4i**	−6.7
10	**4j**	−6.1
11	Ascorbic acid	−5.1
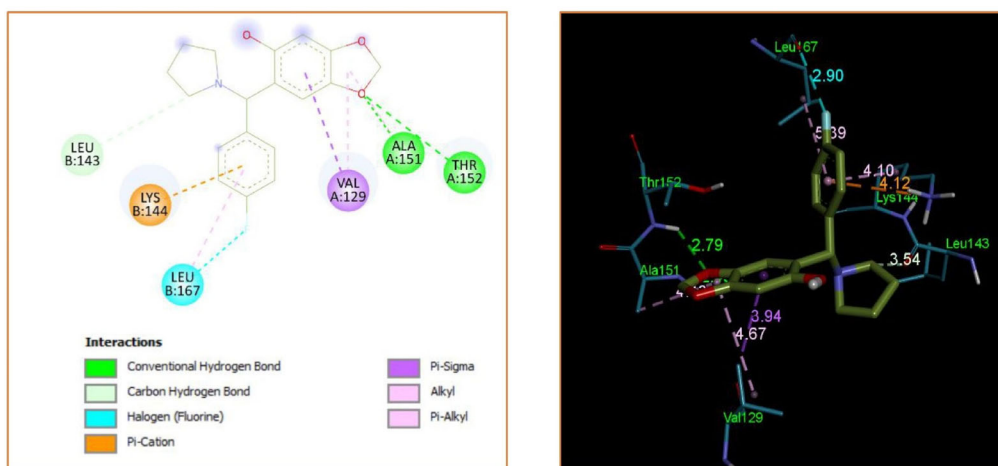
Figure 3. Docked view of compound **4h** at the site of the protein 1PRX.

enzyme 1PRX using autodock vina tool. The predicted docking scores are listed in Table 3. Compounds **4a**, **4f**, and **4h** possess a good docking score. Especially Compound **4 h** showed interaction toward ALA and THR amino acid with conventional hydrogen bond additionally, fluorine interacts with LEU amino acid (Figure 3).

Table 4. Simulation results of compounds **4a–j.**

Entry	Compounds	HOMO (ev)	LUMO (ev)	Dipole	Eg
1	**4a**	−0.299	0.111	4.4834	0.410
2	**4b**	−0.298	0.117	3.8381	0.415
3	**4c**	−0.295	0.119	3.5116	0.414
4	**4d**	−0.280	0.119	4.4834	0.399
5	**4e**	−0.312	0.015	7.7839	0.327
6	**4f**	−0.286	0.125	2.3705	0.411
7	**4g**	−0.290	0.124	2.8652	0.416
8	**4h**	−0.286	0.126	2.2382	0.412
9	**4i**	−0.306	0.018	7.7639	0.324

HOMO of **4a**   Eg = 0.410 ev   LUMO of **4a**

HOMO of **4h**   Eg = 0.412 ev   LUMO of **4h**

HOMO of **4f**   Eg = 0.411 ev   LUMO of **4f**

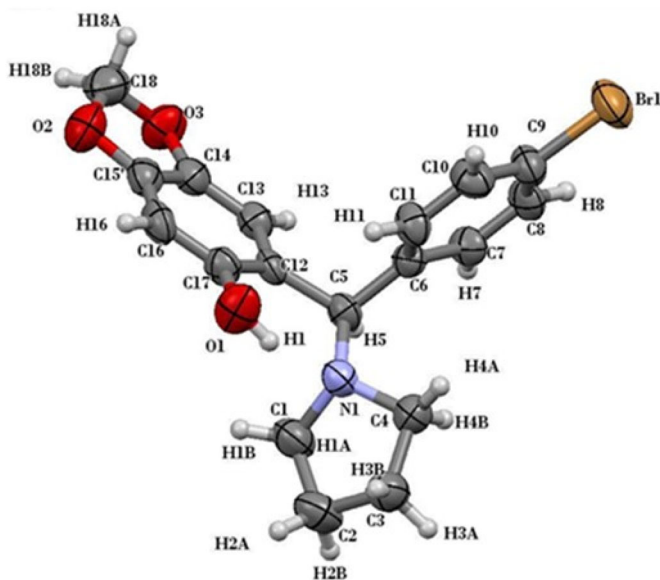**Figure 4.** HOMO, LUMO and Eg of compounds **4a**, **4h,** and **4f**.

Figure 5. ORTEP diagram of compound **4f** (CCDC No. - 2034900).

From the above results, we determined the most potent three compounds (**4a**, **4f**, and **4h**) to correlate the biological response with electronic results. The results of DFT studies are formulated in Table 4. From the results, we may notice that the energy gap of the above-mentioned compounds was low, in particular, the compounds showed good antioxidant properties. The prominent biological action of the motifs (**4a**, **4f**, and **4h**) may be due to their low Eg and docking score as well (Figure 4). Charge transformation may take place easily due to low electron gap and affinity. On the other hand, some of the compounds were low Eg value as comparing the promising compounds however it has a high dock score due to this it can't show excellent antioxidant activity. Many of the compounds (**4c**, **4e**, **4i**, and **4j**) have a high value of Eg as well as dock score as a result they showed the least activity. This may occur due to the high dock score and high value of energy gap as a result charge transformation may be marginal or not possible. The graphical representation is shown in Figure 1 which had shown a correlation between energy gap and dock score.

3.4. Single crystal study

In the title compound, $C_{18}H_{18}BrNO_3$, the five-membered dioxole ring in the molecule has an envelope conformation with the methylene-C18 atom as the flap. The pyrrole ring system adopts an envelope conformation with less torsional strain. The confirmation of the pyrrole ring is described in form of torsion angles of C5-N1-C4-C3 [−164.16 (3)] and C3-C2-C1-N1 [−10.78(3)] respectively indicate higher puckering at N1 compared to C3. The benzodioxole ring and substituted benzene ring occupy an equatorial position and form a dihedral angle of C6-C5-C12 [109.20(7)°], N1-C5-C6 [111.63(7)°] and N1-C5-C12 [111.20(7)°] concerning the main plane of the pyrrole ring system. In the crystal, no specific directional intermolecular interaction is observed. The possible intramolecular hydrogen bonding O1-H1--N1 is observed with 1.844 Å helps to stabilize the molecule. The packing of the molecule in the crystal structures is shown in Figure 5. The result of crystallography is mentioned in Table 5. The data of crystal is deposited in Cambridge Crystallographic Data Center.[46]

Table 5. Crystallographic data and refinement information.

Entry	Chemical formula	$C_{18}H_{18}BrNO_3$
1	Molecular weight	376.23
2	Crystal System	Orthorhombic
3	Space group	$P\ 2_1\ 2_1\ 2_1$
4	Temperature (k)	293
5	Crystal Dimensions (mm)	$0.620 \times 0.400 \times 0.300$
6	a (Å)	8.4620(13)
7	b (Å)	10.4733(16)
8	c (Å)	18.275(3)
9	Cell angles (°)	$\alpha = 90,\ \beta = 90,\ \gamma = 90$
10	V (Å^3)	1619.62
11	Z	4
12	Radiation type	$MoK\alpha\ (\lambda = 0.71073\ Å)$
13	Dcal (gm/cm^3)	1.543
14	μ (mm^{-1})	2.553
15	F (000)	768.00
16	$h, k, l\ max$	11,14,25
17	Diffractometer	Rigaku SCX mini
18	Absorption correction	Multi scan
19	T_{min}, T_{max}	0.638, 0.755
20	2θ	59.01
21	N_{ref}, N_{par}	4535, 209
22	Data completeness	1.49/0.85
23	R, wR_2, S	0.0913, 0.2390, 1.103

4. Conclusion

Synthesis series of sesamol containing derivatives by Betti base synthesis which potent as antioxidant agents. Sesamol is a highly potent antioxidant, further modification can enhance the biological response. Our efforts toward the development of more potent antioxidants. Present work is designed based on theoretical parameters. We synthesized Betti base derivatives with help of the green chemistry principle and it was carried out under aqueous conditions. After, all synthesized molecules were evaluated for their free radical scavenging capacity. Among them compounds **4a**, **4h**, and **4f** had an excellent capacity. In conclusion, the most potent compounds have a good docking score as well as a low value of energy gap.

Disclosure statement

The authors declare no conflict of interest.

ORCID

Jaydeep N. Lalpara 🆔 http://orcid.org/0000-0002-9739-7459
Sanjay D. Hadiyal 🆔 http://orcid.org/0000-0001-7765-6487
Ashoke Sharon 🆔 http://orcid.org/0000-0001-5738-1607
G. G. Dubal 🆔 http://orcid.org/0000-0002-0055-5407

Data availability statement

The data that support the findings of this study are openly available in "figshare" at https://doi.org/10.6084/m9.fig-share.19313951.

References

1. K. Apel, and H. Hirt, "Reactive Oxygen Species: metabolism, Oxidative Stress, and Signal Transduction," *Annual Review of Plant Biology* 55 (2004): 373–99. doi:10.1146/annurev.arplant.55.031903.141701.
2. R. P. Barnes, E. Fouquerel, and P. L. Opresko, "The Impact of Oxidative DNA Damage and Stress on Telomere Homeostasis," *Mechanisms of Ageing and Development* 177 (2019): 37–45. doi:10.1016/j.mad.2018.03.013.
3. H. Schwenzer, F. Juhling, A. Chu, L. J. Pallett, T. F. Baumert, M. Maini, and A. Fassati, "Oxidative Stress Triggers Selective tRNA Retrograde Transport in Human Cells during the Integrated Stress Response," *Cell Reports* 26, no. 12 (2019): 3416–28.e5. −28,doi:10.1016/j.celrep.2019.02.077.
4. R. Mittler, "Oxidative Stress, Antioxidants and Stress Tolerance," *Trends in Plant Science* 7, no. 9 (2002): 405–10. −10,doi:10.1016/S1360-1385(02)02312-9.
5. K. J. Barnham, C. L. Masters, and A. I. Bush, "Neurodegenerative Diseases and Oxidative Stress," *Nature Reviews. Drug Discovery* 3, no. 3 (2004): 205–14. −doi:10.1038/nrd1330.
6. M. T. Lin, and M. F. Beal, "Mitochondrial Dysfunction and Oxidative Stress in Neurodegenerative Diseases," *Nature* 443, no. 7113 (2006): 787–95. doi:10.1038/nature05292.
7. A. Bose, and M. F. Beal, "Mitochondrial Dysfunction and Oxidative Stress in Induced Pluripotent Stem Cell Models of Parkinson's disease," *The European Journal of Neuroscience* 49, no. 4 (2019): 525–32. −32,doi:10.1111/ejn.14264.
8. D. A. Butterfield, and B. Halliwell, "Oxidative Stress, Dysfunctional Glucose Metabolism and Alzheimer Disease," *Nature Reviews. Neuroscience* 20, no. 3 (2019): 148–60. −doi:10.1038/s41583-019-0132-6.
9. D. Giugliano, A. Ceriello, and G. Paolisso, "Oxidative Stress and Diabetic Vascular Complications," *Diabetes Care* 19, no. 3 (1996): 257–67. −doi:10.2337/diacare.19.3.257.
10. E. J. Henriksen, "Role of Oxidative Stress in the Pathogenesis of Insulin Resistance and Type 2 Diabetes," in *Bioactive Food as Dietary Interventions for Diabetes*, 2nd ed., edited by R. R. Watson, and V. R. Preedy, (ScienceDirect, 2019), Chapter 1, 3–17.doi:10.1016/B978-0-12-813822-9.00001-1
11. B. Uttara, A. V. Singh, Paolo Zamboni, and R. T. Mahajan, "Oxidative Stress and Neurodegenerative Diseases: A Review of Upstream and Downstream Antioxidant Therapeutic Options," *Current Neuropharmacology* 7, no. 1 (2009): 65–74. doi:10.2174/157015909787602823.
12. R. S. Sohal, and R. Weindruch, "Oxidative Stress, Caloric Restriction, and Aging," *Science (New York, N.Y.)* 273, no. 5271 (1996): 59–63. doi:10.1126/science.273.5271.59.
13. Finkel Toren, T. Finkel, and N. J. Holbrook, "Oxidants, Oxidative Stress and the Biology of Ageing," *Nature* 408, no. 6809 (2000): 239–47. doi:10.1038/35041687.
14. F. J. Hidalgo, R. M. Delgado, and Rosario Zamora, "Protective Effect of Phenolic Compounds on Carbonyl-Amine Reactions Produced by Lipid-Derived Reactive Carbonyls," *Food Chemistry* 229 (2017): 388–95. doi:10.1016/j.foodchem.2017.02.097.
15. H. Yoshida, and S. Takagi, "Effects of Seed Roasting Temperature and Time on the Quality Characteristics of Sesame (*Sesamum indicum*) Oil," *Journal of the Science of Food and Agriculture* 75, no. 1 (1997): 19–26. doi:10.1002/(SICI)1097-0010(199709)75:1 < 19::AID-JSFA830 > 3.0.CO;2-C.
16. S.-M. Jeong, S.-Y. Kim, D.-R. Kim, K. C. Nam, D. U. Ahn, and S.-C. Lee, "Effect of Seed Roasting Conditions on the Antioxidant Activity of Defatted Sesame Meal Extracts," *Journal of Food Science* 69, no. 5 (2006): C377–81. doi:10.1111/j.1365-2621.2004.tb10701.x.
17. T. Kurechi, K. Kikugawa, and A. Nishizawa, "Transformation of Hemoglobin a into Methemoglobin by Sesamol," *Life Sciences* 26, no. 20 (1980): 1675–81. doi:10.1016/0024-3205(80)90175-7.
18. M. Uchida, S. Nakajin, S. Toyoshima, and M. Shinoda, "Antioxidative Effect of Sesamol and Related Compounds on Lipid Peroxidation," *Biological & Pharmaceutical Bulletin* 19, no. 4 (1996): 623–6. doi:10.1248/bpb.19.623.

19. H. Yoshida, and S. Takagi, "Antioxidative Effects of Sesamol and Tocopherols at Various Concentrations in Oils during Microwave Heating," *Journal of the Science of Food and Agriculture* 79, no. 2 (1999): 220–6. doi: 10.1002/(SICI)1097-0010(199902)79:2 < 220::AID-JSFA173 > 3.0.CO;2-8.

20. H.-S. Hwang, J. K. Winkler-Moser, E. L. Bakota, M. A. Berhow, and S. X. Liu, "Antioxidant Activity of Sesamol in Soybean Oil under Frying Conditions," *Journal of the American Oil Chemists' Society* 90, no. 5 (2013): 659–66. doi:10.1007/s11746-013-2204-5.

21. S. Hong, M.-J. Kim, S. Park, S. Lee, J. Lee, and J. Lee, "Effects of Hydrogen-Donating or Metal-Chelating Antioxidants on the Oxidative Stability of Organogels Made of Beeswax and Grapeseed Oil Exposed to Light Irradiation," *Journal of Food Science* 83, no. 4 (2018): 885–91. doi:10.1111/1750-3841.14085.

22. R. Joshi, M. S. Kumar, K. Satyamoorthy, M. K. Unnikrisnan, and Tulsi Mukherjee, "Free Radical Reactions and Antioxidant Activities of Sesamol: pulse Radiolytic and Biochemical Studies," *Journal of Agricultural and Food Chemistry* 53, no. 7 (2005): 2696–703. doi:10.1021/jf0489769.

23. K. A. Keene, R. M. Ruddy, and M. J. Fhaner, "Investigating the Relationship between Antioxidants and Fatty Acid Degradation Using a Combination Approach of GC-FID and Square-Wave Voltammetry," *ACS Omega* 4, no. 1 (2019): 983–91. doi:10.1021/acsomega.8b02275.

24. A. Chennuru, and M. T. S. Saleem, "Antioxidant, Lipid Lowering, and Membrane Stabilization Effect of Sesamol against Doxorubicin-Induced Cardiomyopathy in Experimental Rats," *BioMed Research International* 20132013, (2013): 934239. doi:10.1155/2013/934239.

25. I. P. Kaur, and A. Saini, "Sesamol Exhibits Antimutagenic Activity against Oxygen Species Mediated Mutagenicity," *Mutation Research* 470, no. 1 (2000): 71–6. doi:10.1016/S1383-5718(00)00096-6.

26. S. Sharma, and I. P. Kaur, "Development and Evaluation of Sesamol as an Antiaging agent," *Int J Dermatol* 45, no. 3 (2006): 200–08. doi:10.1111/j.1365-4632.2004.02537.x.

27. N. R. Prasad, V. P. Menon, V. Vasudev, and K. V. Pugalendi, "Radioprotective Effect of Sesamol on Gamma-Radiation Induced DNA Damage, Lipid Peroxidation and Antioxidants Levels in Cultured Human Lymphocytes," *Toxicology* 209, no. 3 (2005): 225–35. −35, doi:10.1016/j.tox.2004.12.009.

28. A. Kumar, S. Choudhary, J. S. Adhikari, and N. K. Chaudhury, "Sesamol Ameliorates Radiation Induced DNA Damage in Hematopoietic System of Whole Body γ-Irradiated Mice," *Environmental and Molecular Mutagenesis* 59, no. 1 (2018): 79–90. doi:10.1002/em.22118.

29. S. M. Gomha, Z. A. Muhammad, H. M. Abdel-Aziz, I. K. Matar, and A. A. El-Sayed, "Green Synthesis, Molecular Docking and Anticancer Activity of Novel 1,4-Dihydropyridine-3,5-Dicarbohydrazones under Grind-Stone Chemistry," *Green Chemistry Letters and Reviews* 13, no. 1 (2020): 6–17. no doi:10.1080/17518253.2019.1710268.

30. S. M. Gomha, H. M. Abdel-Aziz, T. Z. Abolibda, S. A. Hassan, and M. M. Abdalla, "Green Synthesis, Molecular Docking and Pharmacological Evaluation of New Triazolo-Thiadiazepinylcoumarine Derivatives as Sedative-Hypnotic Scaffold," *Journal of Heterocyclic Chemistry* 57, no. 3 (2020): 1034–43. doi:10.1002/jhet.3827.

31. K. D. Khalil, S. M. Riyadh, S. M. Gomha, and I. Ali, "Synthesis, Characterization and Application of Copper Oxide Chitosan Nanocomposite for Green Regioselective Synthesis of [1,2,3]triazoles," *International Journal of Biological Macromolecules* 130, no. 1 (2019): 928–37. [1,2,3]triazoles,"doi:10.1016/j.ijbiomac.2019.03.019.

32. S. M. Gomha, M. R. Abdelaziz, H. M. Abdel-Aziz, and S. A. Hassan, "Green Synthesis and Molecular Docking of Thiazolyl-Thiazole Derivatives as Potential Cytotoxic Agents," *Mini Reviews in Medicinal Chemistry* 17, no. 9 (2017): 805–15. doi:10.2174/1389557516666161223154539.

33. A. J. Radia, J. N. Lalpara, I. J. Modasiya, and G. G. Dubal, "Design and Synthesis of Novel 1,3,4-Oxadiazole Based Azaspirocycles Catalyzed by NaI under Mild Condition and Evaluated Their Antidiabetic and Antibacterial Activities," *Journal of Heterocyclic Chemistry* 58, no. 2 (2021): 612–21. doi:10.1002/jhet.4200.

34. S. D. Hadiyal, N. D. Parmar, P. L. Kalavadiya, J. N. Lalpara, and H. S. Joshi, "Microwave-Assisted Three-Component Domino Synthesis of Polysubstituted 4*H*-Pyran Derivatives and Their Anticancer Activity," *Russian Journal of Organic Chemistry* 56, no. 4 (2020): 671–8. doi:10.1134/S1070428020040168.

35. J. N. Lalpara, M. D. Vachhani, S. D. Hadiyal, S. Goswami, and G. G. Dubal, "Synthesis and in Vitro Antidiabetic Screening of Novel Dihydropyrimidine Derivatives," *Russian Journal of Organic Chemistry* 57, no. 2 (2021): 241–6. doi:10.1134/S1070428021020159.

36. S. D. Hadiyal, J. N. Lalpara, N. D. Parmar, and H. S. Joshi, "Microwave Irradiated Targeted Synthesis of Pyrrolobenzodiazepine Embrace 1,2,3-Triazole by Click Chemistry Synthetic Aspect and Evaluation of Anticancer and Antimicrobial Activity," *Polycyclic Aromatic Compounds* (2021): 1–17. (Advance online publication), doi:10.1080/104066381913425.

37. J. N. Lalpara, S. D. Hadiyal, A. J. Radia, J. M. Dhalani, and G. G. Dubal, "Design and Rapid Microwave Irradiated One-Pot Synthesis of Tetrahydropyrimidine Derivatives and Their Screening in Vitro Antidiabetic Activity," *Polycyclic Aromatic Compounds* (2020): 1–15. (Advance online publication), doi:10.1080/104066381852586.

38. M. Burits, and F. Bucar, "Antioxidant Activity of Nigella Sativa Essential Oil," *Phytotherapy Research* 14, no. 5 (2000): 323–8. doi:10.1002/1099-1573(200008)14:5 < 323::AID-PTR621 > 3.0.CO;2-Q.
39. M. Cuendet, K. Hostettmann, O. Potterat, and W. Dyatmiko, "Iridoid Glucosides with Free Radical Scavenging Properties from Fagraea Blumei," *Helvetica Chimica Acta* 80, no. 4 (1997): 1144–52. doi:10.1002/hlca.19970800411.
40. R. J. Ruch, S. J. Cheng, and J. E. Klaunig, "Prevention of Cytotoxicity and Inhibition of Intercellular Communication by Antioxidant Catechins Isolated from Chinese Green Tea," *Carcinogenesis* 10, no. 6 (1989): 1003–8. doi:10.1093/carcin/10.6.1003.
41. L. C. Green, D. A. Wagner, J. Glogowski, P. L. Skipper, J. S. Wishnok, and S. R. Tannenbaum, "Analysis of Nitrate, Nitrite, and [^{15}N] Nitrate in Biological Fluids," *Analytical Biochemistry* 126, no. 1 (1982): 131–8. 38, doi:10.1016/0003-2697(82)90118-X.
42. L. Marcocci, J. J. Maguire, M. T. Droy-Lefaix, and L. Packer, "The Nitric Oxide-Scavenging Properties of Ginkgo Biloba Extract EGb 761," *Biochemical and Biophysical Research Communications* 201, no. 2 (1994): 748–55. doi:10.1006/bbrc.1994.1764.
43. O. Trott, and A. J. Olson, "AutoDock Vina: Improving the Speed and Accuracy of Docking with a New Scoring Function, Efficient Optimization, and Multithreading," *Journal of Computational Chemistry* 31, no. 2 (2010): 455–61. doi:10.1002/jcc.21334.
44. G. Gece, "The Use of Quantum Chemical Methods in Corrosion Inhibitor Studies," *Corrosion Science* 50, no. 11 (2008): 2981–92. doi:10.1016/j.corsci.2008.08.043.
45. A. Altomare, G. Cascarano, C. Giacovazzo, A. Guagliardi, M. C. Burla, G. Polidori, and M. Camalli, "SIR92 - a Program for Automatic Solution of Crystal Structures by Direct Methods," *Journal of Applied Crystallography* 27, no. 3 (1994): 435. 435, doi:10.1107/S002188989400021X.
46. CCDC 2034900 contains the supplementary crystallographic data for compound 2h. The data can be obtained free of charge from The Cambridge Crystallographic Data Centre via http://www.ccdc.cam.ac.uk/getstructures, doi: 10.5517/ccdc.csd.cc269gyy.